APPLIED AND ENVIRONMENTAL MICROBIOLOGY, June 1990, p. 1636–1644
0099-2240/90/061636-09$02.00/0
Copyright © 1990, American Society for Microbiology
Vol. 56, No. 6

# Liquid-to-Gas Mass Transfer in Anaerobic Processes: Inevitable Transfer Limitations of Methane and Hydrogen in the Biomethanation Process

ANDRÉ PAUSS, GÉRALD ANDRE, MICHEL PERRIER, AND SERGE R. GUIOT*

*Biotechnology Research Institute, National Research Council Canada, 6100 Avenue Royalmount, Montréal, Québec H4P 2R2, Canada*

Received 15 August 1989/Accepted 26 March 1990

**Liquid-to-gas mass transfer in anaerobic processes was investigated theoretically and experimentally. By using the classical definition of $k_La$, the global volumetric mass transfer coefficient, theoretical development of mass balances in such processes demonstrates that the mass transfer of highly soluble gases is not limited in the usual conditions occurring in anaerobic fermentors (low-intensity mixing). Conversely, the limitation is important for poorly soluble gases, such as methane and hydrogen. The latter could be overconcentrated to as much as 80 times the value at thermodynamic equilibrium. Such overconcentrations bring into question the biological interpretations that have been deduced solely from gaseous measurements. Experimental results obtained in three different methanogenic reactors for a wide range of conditions of mixing and gas production confirmed the general existence of low mass transfer coefficients and consequently of large overconcentrations of dissolved methane and hydrogen (up to 12 and 70 times the equilibrium values, respectively). Hydrogen mass transfer coefficients were obtained from the direct measurements of dissolved and gaseous concentrations, while carbon dioxide coefficients were calculated from gas phase composition and calculation of related dissolved concentration. Methane transfer coefficients were based on calculations from the carbon dioxide coefficients. From mass balances performed on a gas bubble during its simulated growth and ascent to the surface of the liquid, the methane and carbon dioxide contents in the gas bubble appeared to be controlled by the bubble growth process, while the bubble ascent was largely responsible for a slight enrichment in hydrogen.**

The theory of liquid-to-gas or gas-to-liquid mass transfer in biological processes has been developed in numerous engineering textbooks (e.g., references 1 and 19). Applications have been, however, essentially restricted to oxygen transfer in aerobic processes. In anaerobic processes in which many different gases (such as methane, nitrogen, hydrogen, hydrogen sulfide, and carbon dioxide) are produced and/or consumed, the problem of liquid-to-gas transfer is quite poorly documented. Generally, material balances on these species assume equilibrium between phases as dictated by Henry's law.

In the biomethanation process, in which numerous gases are produced, liquid-to-gas transfer is crucial. Methane, carbon dioxide, hydrogen, and hydrogen sulfide gases result from the activity of microorganisms in the liquid phase. Thermodynamic considerations about dissolved hydrogen interspecies transfer, as well as carbon balances around a reactor based on methane flow rates or specific microbial production and/or consumption rates, are subject to error when interphase transfer resistance is neglected. On the other hand, hydrogen, an intermediate metabolite in the process, must be present at a very low concentration to ensure the proper operation of the process. For instance, its partial pressure at equilibrium must be no more than 10 Pa to allow degradation of propionate (13). Because of technical difficulties involved in the direct measurement of dissolved hydrogen, most hydrogen techniques have been developed for the gas phase (10); knowledge of possible hydrogen transfer limitations is then crucial for estimating the dissolved $H_2$ concentration. On-line dissolved-hydrogen sensors are now available (14a, 17, 20) to investigate the interphase transfer of hydrogen.

Carbon dioxide was shown to be in quasiequilibrium under normal operating conditions (2), while no data have been reported about methane gas transfer. In studying batch kinetics of consumption of gaseous hydrogen plus carbon dioxide, Robinson and Tiedje (16) found that hydrogen transfer was the limiting step in the case of highly concentrated or viscous sludge. These conclusions were drawn despite an experimental design favoring gas transfer from the gas to the liquid phase, i.e., a gas-to-liquid volume ratio of 3, and strong mixing of the sludge. Fardeau and co-workers (8, 9) have studied the growth of *Methanococcus thermolithotrophicus* and *Methanobacterium thermoautotrophicum* on $H_2$ and $CO_2$ under batch conditions and in continuous culture in fermentors where the agitation rate was low and where the gas transfer was not optimal. When a high agitation speed (up to 1,300 rpm with an impeller) was used in fermentors operated in batch mode, the methane productivity and the final biomass concentration were increased 17- and 4-fold, respectively, compared with earlier experiments. Their results clearly indicated that the level of dissolved hydrogen was the growth-limiting factor in this fermentation (15). Other preliminary results, recently presented by Jud et al. (FEMS Symposium, Marseille, France, 12 to 14 September, 1989), also indicated hydrogen mass transfer limitations in a culture of *M. thermoautotrophicum* growing on $H_2$ and $CO_2$.

We report here the results of experiments in anaerobic fermentors of different designs and operated under various conditions for which the liquid and gas phase concentrations were compared; the resulting mass transfer limitations are discussed.

* Corresponding author.

Before the experimental results are discussed, theoretical material balances involving mass transfer terms are presented below to facilitate understanding of the phenomenon. The mathematical approach used is not restricted to the biomethanation process and could be easily extended to other multiphase bioreactors.

## THEORY

**Nomenclature.** The following variables and abbreviations will be used throughout this paper: biol. rate, net volumetric rate of production due to biological activity (moles liter$^{-1}$ hour$^{-1}$); $D$, gas diffusivity coefficient (centimeters$^2$ second$^{-1}$); D, dilution rate (hour$^{-1}$); HRT, hydraulic retention time (days); $K_H$, Henry's law constant (moles liter$^{-1}$ pascal$^{-1}$); $k_La$, global volumetric mass transfer coefficient for the bioreactor (hour$^{-1}$); OLR, organic loading rate (grams$_{COD}$ liter$^{-1}$ day$^{-1}$ [COD, chemical oxygen demand]); $p_{gas}$, gas partial pressure (pascals); phys. rate, net volumetric rate of production due to physicochemical reaction, i.e., pH variation (moles liter$^{-1}$ hour$^{-1}$); $Q_g$, gas flow rate (liters hour$^{-1}$); $Q_V$, volumetric gas production rate ($Q_g/V_L$); $R$, ideal gas constant (8,314 Pa mole$^{-1}$ K$^{-1}$); $T$, temperature (Kelvin); $V_L$, volume of the liquid phase (liters); $V_g$, volume of the gas phase (liters); $[gas]_g$, concentration of gaseous species in the gas phase (moles liter$^{-1}$); $[gas]_{L,in}$, concentration of dissolved gaseous species in the influent (moles liter$^{-1}$); $[gas]_{L,ef}$, concentration of dissolved gaseous species in the effluent (moles liter$^{-1}$); $[gas]_L$, concentration of dissolved gaseous species in the reactor (normally equal to the concentration in the effluent) (moles liter$^{-1}$); $[gas]_L^*$, concentration of dissolved gaseous species in the reactor at thermodynamic equilibrium (moles liter$^{-1}$) (equal to $p_{gas} \times K_H$); $[gas]_L/[gas]_L^*$, overconcentration factor.

**Anaerobic processes.** When a continuously fed fermentor and homogeneous gas and liquid phases are considered, mass balances of gaseous metabolites can be established for both liquid and gas phases:

for the liquid phase,

$$\frac{d[gas]_L}{dt} = D([gas]_{L,in} - [gas]_{L,ef}) + \text{(biological rate)} + \text{(physicochemical rate)} - k_La([gas]_L - [gas]_L^*) \quad (1)$$

for the gas phase,

$$\frac{d[gas]_g}{dt} = \frac{V_L}{V_g} k_La([gas]_L - [gas]_L^*) - \frac{Q_g p_{gas}}{V_g RT} \quad (2)$$

In equations 1 and 2, the driving force for the transfer from the liquid phase to the gas phase is expressed as the difference between the actual concentration of dissolved gas and the concentration that would be in equilibrium with the partial pressure of the given species in the gas phase.

The global mass transfer coefficient, $k_La$, is representative of the rate of transfer in either direction (gas to liquid or liquid to gas) for the whole reactor. Conceptually, $k_La$ is made up of two terms, $k_L$ (the "film" coefficient) and $a$ (the specific interfacial area per unit volume of liquid in the reactor). $k_La$ is usually determined as a single coefficient from experimental data and is clearly specific to a given reactor and mode of operation. $k_L$ is a function of the nature of the gas and of the physicochemical properties of the liquid phase, whereas $a$ is largely dependent on the hydrodynamic conditions existing in the bioreactor and on the gas production rate. In anaerobic reactors in which bubbles occur as a result of internal biological activities, it is expected that $a$ (and thus $k_La$) will be greatly influenced by the bubble formation process and gas production rate. Mixing of the liquid phase will be less important as long as the concentrations of the various species are kept uniform.

TABLE 1. Physical data of the different gases of a biomethanation process

| Gas | Diffusivity coefficient[a] ($D$) (cm$^2$/s$^{-1}$) ($10^5$) | Henry's constant[b] ($K_H$) (mol liter$^{-1}$ Pa$^{-1}$) |
|---|---|---|
| $H_2$ | 4.65 | $7.40 \times 10^{-9}$ |
| $CH_4$ | 1.57 | $1.12 \times 10^{-8}$ |
| $CO_2$ | 1.98 | $2.70 \times 10^{-7}$ |
| $H_2S$ | NA[c] | $8.22 \times 10^{-7}$ |

[a] From Sherwood et al. (19).
[b] From Seidell (18).
[c] NA, Not available.

At a steady state, the above equations can be easily solved. A steady state corresponds to the situation where the observed parameters (namely, composition of the gas phase, dissolved metabolite concentration, and dissolved gas concentration) are constant. In such conditions, the time derivatives are set to zero, and by introducing the volumetric gas production rate, $Q_v = Q_g/V_L$ (liters of gas liters of reactor$^{-1}$ hour$^{-1}$), equation 2 becomes

$$k_La = \frac{Q_v}{K_HRT\left(\frac{[gas]_L}{[gas]_L^*} - 1\right)} \quad (3)$$

or

$$\frac{[gas]_L}{[gas]_L^*} - 1 = \frac{Q_v}{K_HRTk_La} \quad (4)$$

A steady state with no mass transfer limitation is characterized by a dissolved-gas concentration very close to the equilibrium value, i.e., $[gas]_L/[gas]_L^* \approx 1$. In this case, $k_La$ approaches infinity, which means that the controlling resistance is the production process (in practice, the actual dissolved-gas concentration will always be greater than the value at equilibrium).

Equation 4 also indicates that, for a given volumetric gas production rate and for a fixed value of the mass transfer coefficient, the $[gas]_L/[gas]_L^*$ ratio approaches 1 (i.e., thermodynamic equilibrium) in the case of more soluble gases, i.e., high $K_H$ values (Table 1). Highly soluble gases, such as $CO_2$, $H_2S$, and $NH_3$, are more likely to be at thermodynamic equilibrium even for a low $k_La$ value, while poorly soluble gases, such as $O_2$, $N_2$, $H_2$, and $CH_4$, are predicted to be further away from thermodynamic equilibrium. The variations of the overconcentration factor ($[gas]_L/[gas]_L^*$) of four different gases as a function of the mass transfer coefficient are shown in Fig. 1. For a volumetric gas production rate of 1 liter of gas per liter of reactor per day ($Q_v$) at 35°C, the transfer coefficients for $H_2$ and $CH_4$ lower than 22 and 14.5 h$^{-1}$, respectively, will result in an overconcentration of these gases with respect to thermodynamic equilibrium. On the other hand, the $k_La$ coefficients of $CO_2$ and $H_2S$ are approximately 2 orders of magnitude lower.

**The biomethanation process.** Applying the above analysis

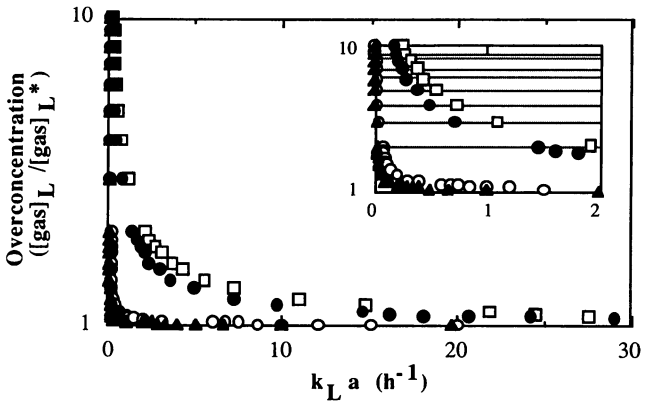


FIG. 1. Overconcentration of gases in the liquid phase as a function of their mass transfer coefficient (at 35°C; $Q_v$ = 1 liter of gas liter$^{-1}$ day$^{-1}$). Inset, Magnification of the gas overconcentration variations for $k_La$ values between 0 and 2 h$^{-1}$. Symbols: □, $H_2$; ●, $CH_4$; ○, $CO_2$; ▲, $H_2S$.

to the biomethanation process, in which methane, carbon dioxide, hydrogen, and hydrogen sulfide gases are involved, overconcentrations of methane and hydrogen (both poorly soluble gases) in the liquid phase can be anticipated. This problem deserves consideration for the following four reasons. First, as the mass transfer coefficient of gases is mostly affected by design and operating parameters (such as mixing efficiency, reactor design, and specific total gas production rate), $k_La$'s should be of the same order of magnitude for all gases. In fact, $k_La$ is slightly affected by the properties of the gaseous species, as $k_L$ varies with the square root of the diffusivity (6). Second, mixing intensity in methanogenic reactors is generally just high enough to homogenize the liquid phase, but it is presumably limited to preserve the syntrophic associations of microorganisms. Third, mixing problems often occur in full-scale reactors. Demuynck et al. (7), for example, showed that 20% of the full-scale methanogenic reactors surveyed in the European Community present major or minor mixing problems. Fourth, as shown in equation 4, the higher the volumetric gas rate, i.e., as in almost all industrial-scale reactors, the higher the expected overconcentration of dissolved gas in the liquid for a given $k_La$.

The theoretical developments described above thus clearly demonstrate that anaerobic processes, and more particularly the biomethanation process, could suffer from severe liquid-to-gas transfer limitations. In the next section, we will evaluate the importance of such phenomena in real methanogenic reactors.

## MATERIALS AND METHODS

**Experimental protocol.** To evaluate the importance of mass transfer limitations in real anaerobic reactors, the dissolved hydrogen concentrations were compared with the gaseous hydrogen measurements in three reactors of different designs: a completely stirred reactor, an upflow sludge bed reactor, and an upflow sludge bed reactor topped with a filter part (UBF reactor). Different steady-state conditions or batch conditions were applied to these reactors to obtain the widest possible range of hydraulic and biological conditions: mechanical agitation or liquid recycle, low and high hydraulic retention times, and low and high gas production rates (Table 2).

Our experimental protocol focused on hydrogen and methane, as they were expected to be the gases most sensitive to mass transfer limitations. During at least two residence times (from 2 to 38 days, depending on the reactor), the hydrogen and methane fractions of the gas phase and the total gas flow rate were measured daily, while the dissolved hydrogen level was continuously recorded. Average values were used to calculate the transfer coefficients, namely, the $H_2$ transfer rate and the $H_2$ overconcentration factor (equation 3). Assuming that the mass transfer coefficients of the different gases in the medium are proportional to the square root of their diffusivity (equation 5), the $k_La$ value and then the overconcentration factor of $CH_4$ were calculated for the three reactors on the basis of hydrogen data.

$$(k_La)_{CH_4} = (k_La)_{H_2} (D_{CH_4}/D_{H_2})^{1/2} \quad (5)$$

Finally, for each gas species, both terms which describe the removal rate from the reactor (equation 1) were compared. These terms are the loss in the effluent (D $[gas]_L$) and the interphase transfer rate $\{k_La([gas]_L - [gas]_L^*)\}$.

**Reactors.** The baffled, Plexiglas-built, completely stirred reactor was operated in a fed-batch mode. For 20 h each day, the reactor was continuously fed while agitation of the liquid was maintained, thereby increasing the liquid volume from 21 to 32.5 liters. To keep the biomass in the reactor, the mixing and the feed addition were stopped for 4 h each day. A total of 11.5 liters of decanted liquid was then removed for the next cycle (an average liquid volume of 26.75 liters was used for the calculations of volumetric parameters). A concentrated synthetic medium was diluted with bicarbonate-buffered tap water ($NaHCO_3$ [8 g/liter], $KHCO_3$ [10 g/liter]) in a 1/40 (vol/vol) ratio. One liter of the concentrated medium contained sucrose (198 g), ammonium acetate (37 g), potassium acetate (47 g), sodium acetate (39 g), yeast extract (32 g), $KH_2PO_4$ (6.8 g), $K_2HPO_4$ (8.7 g), $NH_4HCO_3$ (33 g), $(NH_4)_2SO_4$ (5 g), $KHCO_3$ (55 g), $NaHCO_3$ (46 g), and 50 ml of a trace metal solution, of which 1 liter contained $FeCl_2 \cdot 4H_2O$ (2 g), $H_3BO_3$ (50 mg), $ZnCl_2$ (50 mg),

TABLE 2. Running conditions for all reactors

| Reactor type and condition | OLR ($g_{COD}$ liter$^{-1}$ day$^{-1}$) | D (day$^{-1}$) ± SD | pH ± SD | $Q_V$ (liters of gas liter$^{-1}$ day$^{-1}$) |
|---|---|---|---|---|
| Completely stirred | 5.70 | 0.43 ± 0.02 | 7.77 ± 0.05 | 2.39 ± 0.18 |
| Sludge bed | | | | |
| Steady state 1 | 1.20 | 0.081 ± 0.001 | 7.6 ± 0.1 | 0.64 ± 0.4 |
| Steady state 2 | 1.57 | 0.053 ± 0.001 | 7.44 ± 0.03 | 0.95 ± 0.05 |
| UBF | | | | |
| Steady state 1 | 27.0 | 3.0 ± 0.4 | 7.22 ± 0.02 | 9.3 ± 1.4 |
| Steady state 2 | 7.50 | 2.2 ± 0.2 | 7.12 ± 0.05 | 1.73 ± 0.06 |

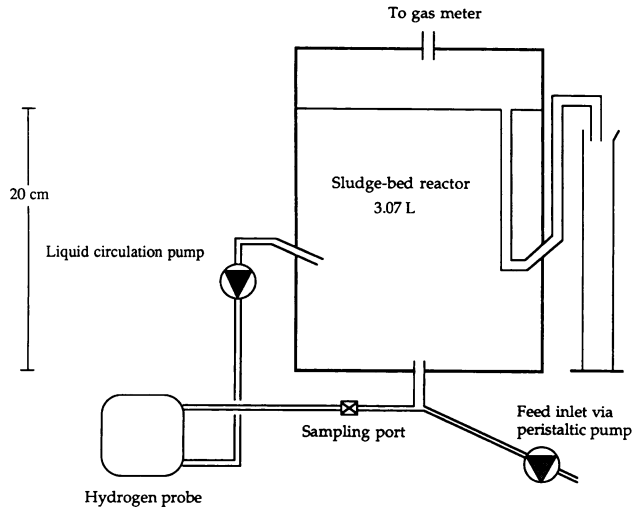


FIG. 2. Schematic of the sludge bed reactor.

$CuCl_2 \cdot 2H_2O$ (40 mg), $MnCl_2 \cdot 4H_2O$ (500 mg), $(NH_4)_6 Mo_7O_{24} \cdot 4H_2O$ (50 mg), $AlCl_3$ (30 mg), $CoCl_2 \cdot 6H_2O$ (150 mg), $NiCl_2 \cdot 6H_2O$ (100 mg), disodium EDTA salt dihydrate (500 mg), and 1 ml of concentrated HCl. The mixing was done by a vertical "Möbius-ribbon"-like paddle rotated at 400 rpm by a dual-shaft variable-speed stirrer (Cole-Parmer). The reactor was maintained at 35°C. The gas production was measured with an automated pressure transducer gas meter (3).

The sludge-bed reactor had a working volume of 3.07 liters (Fig. 2). It was fed continuously with a synthetic medium dissolved in tap water. This was composed of $NH_4HCO_3$ (3.6 g/liter), $NaHCO_3$ (8.4 g/liter), $KHCO_3$ (10.0 g/liter), $(NH_4)_2SO_4$ (0.3 g/liter), and $KH_2PO_4$ (0.6 g/liter) for both steady states plus sucrose (12.5 [first] and 25 g/liter [second]) and yeast extract (0.5 [first] and 1 g/liter [second]) for the first and the second steady states. Mixing was ensured by the recirculation of the supernatant liquid through the dissolved-hydrogen probe at a flow rate of 250 ml/min, corresponding to an upflow velocity of 0.85 m/h and to recirculation/feed ratios of 1,440 and 2,200, respectively, for the first and the second steady states. The reactor was maintained at 32°C. The gas production was measured with an automated pressure transducer gas meter (3).

The upflow sludge-bed filter reactor (UBF reactor) had a working volume of 13.4 liters (Fig. 3). It was continuously fed with a concentrated synthetic medium and bicarbonate-buffered tap water in ratios of 1/47 and 1/127 (vol/vol), respectively, for the first and second steady states. The concentrated medium contained sucrose (380 g), yeast extract (3.8 g), $KH_2PO_4$ (7.6 g), $K_2HPO_4$ (10 g), $(NH_4)_2SO_4$ (19 g), and $NH_4HCO_3$ (76 g) per kg of tap water. The bicarbonate-buffered tap water contained $NaHCO_3$ (10 [first] and 4 g/liter [second]) and $KHCO_3$ (12.5 [first] and 5 g/liter [second]) for the first and second steady states. The liquid was continuously recirculated to ensure an upflow velocity of 0.9 m/h and a recirculation/feed ratio of 10.5 (the pump was obtained from pump Jabsco). The reactor was maintained at 35°C, and gas production was recorded with a Wet Tip Gas Meter. The supernatant liquid was continuously circulated at 250 ml/min through a Syprotec cell to measure the dissolved-hydrogen concentration.

**Analytical procedures.** The analytical procedures are described in detail by Pauss et al. (14a). Acetate and propionate

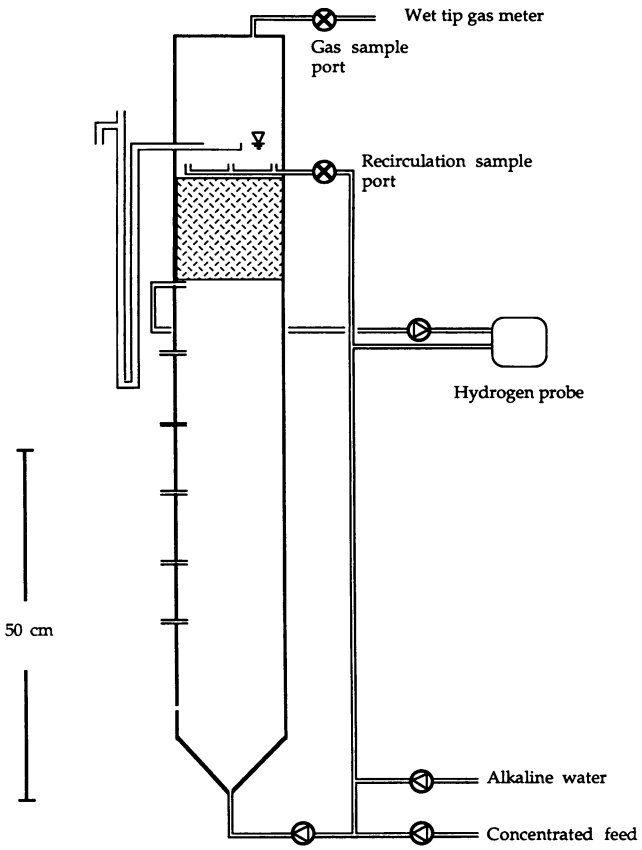


FIG. 3. Schematic of the UBF reactor.

were determined by gas-liquid chromatography of free acids, obtained by adding 1 volume of 6% (wt/vol) formic acid to 1 volume of centrifuged sample. Methane and carbon dioxide gas fractions were analyzed via gas chromatography with a thermal conductivity detector. The hydrogen gas fraction was determined by gas chromatography with thermal conductivity detection and with nitrogen gas as a carrier. With a 1-ml sample loop, the detection limit was about 3 Pa (30 ppm [30 μl/liter]). Dissolved hydrogen was continuously quantified with a probe (Syprotec, Pointe-Claire, Québec, Canada). The detection limit of dissolved hydrogen was 80 nmol/liter. The pH was measured with a combined Radiometer electrode. The chemical oxygen demand (COD) was determined colorimetrically by the method of Knechtel (11).

## RESULTS

**Completely stirred reactor.** The completely stirred reactor was operated in a fed-batch mode in most cases, as previously described, but some results were also obtained in a batch mode. The resulting output coefficients of the first operating mode are shown in Table 3. In spite of a good mixing of the liquid phase (i.e., paddle rotation at 400 rpm in the baffled reactor), large hydrogen and methane overconcentrations were observed in the liquid phase (35 and 39 times the equilibrium values, respectively), and the resulting $k_La$ values were found to be quite low (0.16 and 0.09 $h^{-1}$, respectively).

In the second operating mode (batch mode), the hydrogen concentration and partial pressure were recorded during propionate degradation. The propionate degradation, the

TABLE 3. Performance of the completely stirred reactor at a steady state

| Gas[a] | Parameter[b] | | | |
|---|---|---|---|---|
| | $k_La$ ± SD ($h^{-1}$) | $[gas]_L/[gas]_L^*$ ± SD | D$[gas]_L$ ± SD | $k_La([gas]_L - [gas]_L^*)$ ± SD |
| $H_2$ | 0.16 ± 0.02 | 35 ± 2 | 35.8 ± 3.6 nmol $h^{-1}$ (10% of flux)[c] | 300 ± 60 nmol $h^{-1}$ (90% of flux) |
| $CH_4$ | 0.09 ± 0.01 | 39 ± 7 | 0.44 ± 0.11 mmol $h^{-1}$ (17% of flux) | 2.2 ± 0.6 mmol $h^{-1}$ (83% of flux) |

[a] Dissolved $H_2$ concentration was 2 ± 0.1 μM. $p_{H_2}$, 7.8 ± 0.1 Pa; $p_{CH_4}$, 56.2 ± 0.5 kPa.
[b] $k_La$ for $H_2$ resulted from dissolved and gaseous $H_2$ measurements. Dissolved $CH_4$ concentration and $k_La$ for $CH_4$ were predicted from the data for $H_2$.
[c] Percentage of total gas flux escaping the reactor in the effluent and in the gas phase.

gaseous and dissolved hydrogen concentrations, and the resulting overconcentration and mass transfer coefficients with time are shown in Fig. 4 and 5. The liquid volume was continuously mixed during this experiment. Again, the results indicated large mass transfer limitations. The lower $k_La$ values compared with the steady-state data (obtained just before the batch experience) can be attributed to a lower gas production rate (from 0.7 to 0.25 compared with 2.39 liters of gas $liter^{-1}$ $day^{-1}$).

**Sludge bed reactor.** The sludge bed reactor was operated with long hydraulic retention times and low organic loading rates. Low amounts of gas were produced, and thus the mixing mostly originated from the upflow liquid recirculation. Two steady-state periods were considered. The average output coefficients and the mass transfer coefficients for both steady states are shown in Table 4. Low $k_La$ values and important overconcentration factors for methane and hydrogen were also found in this reactor. The slightly better mass transfer rate obtained during the second steady state is explained by a higher gas production rate, leading to a lower dissolved-hydrogen value. Values obtained in the second steady state were more reliable than in the first one because of less scatter in the gas composition data. The analytical method was optimized after the first steady state.

**UBF reactor.** The UBF reactor was operated with short hydraulic retention times and high organic loading rates. Two steady states, characterized by high dissolved-hydrogen concentrations (8.1 and 18.8 μM), were considered for the mass transfer analysis.

As for the two other reactors, low $k_La$ values and high overconcentrations of gases in the liquid (up to 80) were obtained (Table 5). When both steady states were compared, the mass transfer rate seemed to benefit from an increase in the gas production rate in spite of the concomitant increase of hydrogen concentration. Steady state 1 was characterized by a significantly higher rate of hydrogen production, which was accompanied by a lower methane content in the gas. This was due to the inhibitory running conditions used (organic loading rate, 27 $g_{COD}$ $liter^{-1}$ $day^{-1}$). On the other hand, the importance of mass transfer limitations was emphasized with the second steady state, and contrary to all other experiments reported here, the portion of hydrogen and methane which was leaving the reactor in the effluent

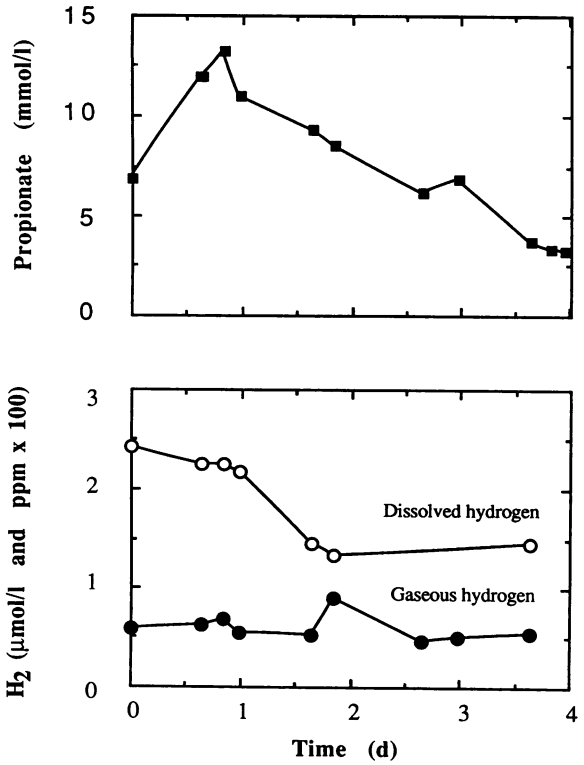


FIG. 4. Metabolite variations during the batch experiment in the completely stirred reactor.

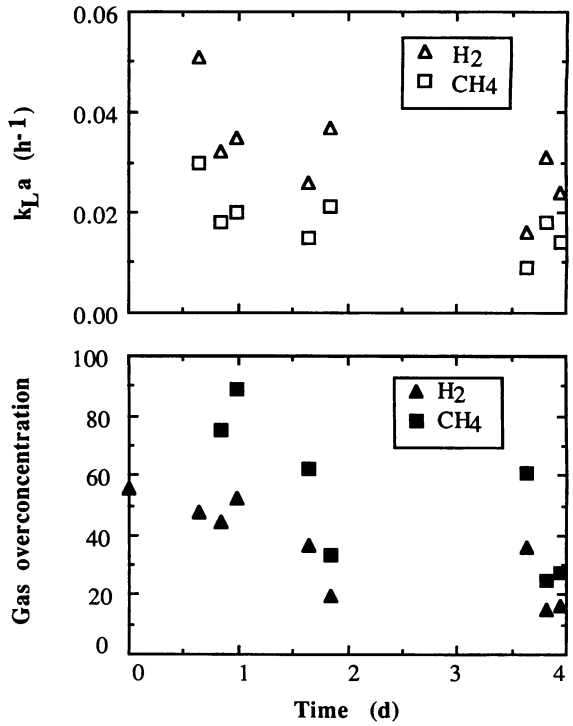


FIG. 5. Course of mass transfer rates during the batch experiment in the completely stirred reactor. ($H_2$, experimental; $CH_4$, predicted by using equations 3 and 5).

TABLE 4. Performance of the sludge bed reactor at both steady states

| Gas | Parameter[a] | | | |
|---|---|---|---|---|
| | $k_La$ ± SD ($h^{-1}$) | $[gas]_L/[gas]_L^*$ ± SD | $D[gas]_L$ ± SD | $k_La([gas]_L - [gas]_L^*)$ ± SD |
| Steady state 1[b] | | | | |
| $H_2$ | 0.03 ± 0.02 | 56 ± 30 | 9.3 ± 2.5 nmol $h^{-1}$ (12% of flux)[c] | 70 ± 50 nmol $h^{-1}$ (88% of flux) |
| $CH_4$ | 0.02 ± 0.01 | 61 ± 50 | 0.12 ± 0.1 mmol $h^{-1}$ (19% of flux) | 0.5 ± 0.4 mmol $h^{-1}$ (81% of flux) |
| Steady state 2[d] | | | | |
| $H_2$ | 0.06 ± 0.03 | 38 ± 15 | 3.3 ± 0.9 nmol $h^{-1}$ (4% of flux) | 82 ± 30 nmol $h^{-1}$ (96% of flux) |
| $CH_4$ | 0.03 ± 0.01 | 41 ± 3 | 0.05 ± 0.007 mmol $h^{-1}$ (6% of flux) | 0.8 ± 0.3 mmol $h^{-1}$ (94% of flux) |

[a] See Table 3, footnote *b*.
[b] Dissolved $H_2$ concentration was 2.75 ± 0.7 μM. $p_{H_2}$, 6.6 ± 2.5 Pa; $p_{CH_4}$, 47 ± 2 kPa.
[c] See Table 3, footnote *c*.
[d] Dissolved $H_2$ concentration was 1.5 ± 0.4 μM. $p_{H_2}$, 5.3 ± 1 Pa; $p_{CH_4}$, 48 ± 2 kPa.

($D[gas]_L$ term) was found to be significantly higher than the portion escaping in the gas phase {$k_La$ ($[gas]_L - [gas]_L^*$) term}. The small liquid retention time and the low gas production rate contributed to this phenomenon.

## DISCUSSION

It appears from theoretical considerations that the interphase mass transfer limitations for highly soluble gases, such as $CO_2$, $NH_3$, and $H_2S$, are less severe even in systems where low $k_La$s occur. On the other hand, poorly soluble gases, such as $N_2$, $H_2$, and $CH_4$, would require higher transfer coefficients if the phenomenon of overconcentration is to be minimized. In aerobic processes, where oxygen is a nutrient and is continuously sparged into the liquid, transfer limitations imply less dissolved oxygen for the growth of microorganisms. In anaerobic processes, where gaseous species are formed in the liquid phase and tend to escape into the gas phase, transfer limitations imply dissolved-gas concentrations higher than the corresponding values at equilibrium. Such overconcentrations can be detrimental to the biological process, for instance by a possible pH drop if acidic gases, such as $CO_2$ or $H_2S$, are produced or by negative thermodynamic effects if an inhibitory gas, such as $H_2$, is present. Finally, overconcentrations of various gaseous species also bring into question in an unpredictable manner some earlier biological interpretations of the process, based exclusively on gaseous measurements which are easier to obtain (e.g., those in references 4, 5, 12, and 16). For instance, specific activities or kinetic parameters obtained solely from gaseous measurements would be erroneous if mass transfer limitations significantly reduced the rates of interphase transfer.

It is essential that the concentration of poorly soluble gases should be directly measured in the liquid phase rather than being estimated solely from gaseous measurements. The lack of accurate measuring devices with which to do so accounts for the lack of this data in the literature. Dissolved-methane concentrations can be measured with mass spectrometry (17). However, no comparisons between such values and the methane partial pressures in the gas phase have yet been published.

All of the experimental results described in this paper confirm the low liquid-to-gas transfer rates of methane and hydrogen in anaerobic reactors inferred in the first section. In the different reactors, for a wide range of mixing conditions, organic loading rates, and related gas production rates, hydrogen was always found to be much more concentrated than the expected equilibrium value (from 35 to 71 times more concentrated). The values of mass transfer coefficients were found to be very low in this study (from 0.03 to 0.40 $h^{-1}$ for $H_2$ and from 0.02 to 0.23 $h^{-1}$ for $CH_4$). These values are to be compared with the $k_La$ values of 10 to 20 $h^{-1}$ usually encountered in aerobic fermentations (19). The range of operating conditions covered in this study is quite representative of the usual conditions of anaerobic bioreactors. On the other hand, it must be emphasized that the mixing conditions used obviously do not ensure efficient liquid-to-gas transfer rates but are sufficient to homogenize the working liquid volume. In the sludge bed reactor, for instance, tracer studies showed that the active volume represented 96% of the total liquid volume (14a).

An important consequence of such low transfer efficiency is the high amount of dissolved gas in the liquid phase. Therefore, the rate at which dissolved gases escape in the

TABLE 5. Performance of the UBF reactor at both steady states

| Gas[a] | Parameter[a] | | | |
|---|---|---|---|---|
| | $k_La$ ± SD ($h^{-1}$) | $[gas]_L/[gas]_L^*$ ± SD | $D[gas]_L$ ± SD | $k_La([gas]_L - [gas]_L^*)$ ± SD |
| Steady state 1[b] | | | | |
| $H_2$ | 0.40 ± 0.06 | 52 ± 4 | 2.4 ± 0.4 μmol $h^{-1}$ (24% of flux)[c] | 7.4 ± 1.9 μmol $h^{-1}$ (76% of flux) |
| $CH_4$ | 0.23 ± 0.04 | 59 ± 19 | 1 ± 0.6 mmol $h^{-1}$ (35% of flux) | 1.7 ± 1 mmol $h^{-1}$ (65% of flux) |
| Steady state 2[d] | | | | |
| $H_2$ | 0.05 ± 0.008 | 71 ± 8 | 0.76 ± 0.09 μmol $h^{-1}$ (64% of flux) | 0.4 ± 0.1 μmol $h^{-1}$ (36% of flux) |
| $CH_4$ | 0.03 ± 0.005 | 81 ± 16 | 1.9 ± 0.8 mmol $h^{-1}$ (75% of flux) | 0.6 ± 0.4 mmol $h^{-1}$ (25% of flux) |

[a] See Table 3, footnote *b*.
[b] Dissolved $H_2$ concentration was 18.8 ± 0.6 μM. $p_{H_2}$, 49 ± 4 Pa; $p_{CH_4}$, 12 ± 2 kPa.
[c] See Table 3, footnote *c*.
[d] Dissolved $H_2$ concentration was 8.1 ± 0.3 μM. $p_{H_2}$, 15 ± 1 Pa; $p_{CH_4}$ 22 ± 3 kPa.

TABLE 6. Comparison of methane liquid-to-gas transfer calculated from hydrogen and carbon dioxide measurements

| Reactor type and steady state | Gas data used for calculations | $k_La$ of $CO_2$ ($h^{-1}$) ± SD | $k_La$ of $CH_4$ ($h^{-1}$) ± SD | $[CH_4]_L/[CH_4]_L^*$ | Amt of $CH_4$ in effluent (% of flux)[a] |
|---|---|---|---|---|---|
| Sludge bed (second) | $H_2$ | | 0.03 ± 0.01 | 41 ± 3 | 6 |
| | $CO_2$ | 0.14 ± 0.02 | 0.12 ± 0.02 | 12 ± 2 | 2 |
| UBF (first) | $H_2$ | | 0.23 ± 0.04 | 59 ± 19 | 35 |
| | $CO_2$ | 1.68 ± 0.59 | 1.49 ± 0.52 | 10 ± 5 | 9 |

[a] See Table 3, footnote *c*.

effluent can constitute an important fraction of the total reactor output (Tables 3, 4, and 5). In the worst case (the second steady state of the UBF reactor), this fraction can become predominant (62 and 75% for hydrogen and methane, respectively). Such important losses are surprising and warrant additional comments. In this work the hydrogen transfer coefficients were directly obtained from experimental measurements, but the methane transfer coefficients were extrapolated from the hydrogen mass transfer coefficient and the relative diffusivities of both gases. Assuming that dissolved methane in the effluent escapes during the preparation of the samples for analyses (such as the COD analysis of the effluent), a high content of methane in the effluent would lead to a gap in the COD balance of the reactor (COD [introduced] = COD [gas] + COD [effluent] + COD [biomass growth]). This unaccountable portion of the COD balance was never found to be significant (i.e., ≤5%), neither in our reactors nor in the literature, where such a COD unbalance would have been readily noticed. Thus, methane mass transfer does not appear to be simply correlated at the hydrogen mass transfer as shown in equation 5.

To account for this discrepancy, dissolved-methane concentration and mass transfer coefficients were alternatively extrapolated from carbon dioxide data. The $k_La$ of carbon dioxide can be calculated when the $CO_2$ partial pressure and the dissolved-$CO_2$ concentration are known. The latter can be calculated when the pH and bicarbonate concentration in the reactor are known, and this method could be as reliable, if not more reliable, than direct measurement with a $CO_2$ probe. Unfortunately, the dissolved-$CO_2$ concentration calculated in this manner is extremely sensitive to the pH value, which therefore must be measured accurately inside the reactor. A ±0.1 unit error, e.g., a pH of 7.12 or 7.32 instead of the measured value of 7.22, varies the $k_La$ values for $CO_2$ and $CH_4$ from 0.8 to 9.6 $h^{-1}$ and from 0.7 to 8.5 $h^{-1}$, respectively (first steady state in the UBF reactor). Let us consider the two steady states for which pH and bicarbonate concentration data were particularly reliable: 7.44 and 246 mmol $liter^{-1}$, respectively, for the sludge-bed reactor (second steady state) (Table 4), and 7.22 and 244 mmol $liter^{-1}$, respectively, for the UBF reactor (first steady state) (Table 5). The resulting $CO_2$ overconcentration factors were 1.41 and 1.33, respectively. The results of the mass transfer calculations are summarized in Table 6. Compared with the values based on hydrogen data, liquid-to-gas mass transfer coefficients for methane were increased by factors of 4 to 6.5, and this was accompanied by a reduction in the methane losses in the effluent. This fraction ranges from 2 to 9% of the total methane output, which is more acceptable and more consistent with results from the literature. However, even when $CO_2$ data was used to calculate the $k_La$ of $CH_4$, the liquid phase was still much more concentrated in dissolved methane than thermodynamic equilibrium (by a factor of about 10 to 12).

The mass transfer coefficients for $CH_4$ calculated from $CO_2$ data thus appeared to be more realistic and more consistent with the expected behavior of the biomethanation process. Moreover, the $k_La$'s observed for hydrogen were almost 1 order of magnitude smaller than those calculated for carbon dioxide. This contrasts with what would be expected from physical mass transfer considerations alone, since the diffusivity of hydrogen is two to three times higher than that of $CO_2$ (Table 1). All these results suggest that the mechanism of liquid-to-gas transfer is similar for $CH_4$ and $CO_2$ but that this is radically different from the mechanism of $H_2$ mass transfer.

A tentative explanation of those two different mechanisms of liquid-to-gas transfer is given in the Appendix. Basically, the simulated liquid-to-gas mass transfer of a single bubble moving vertically in a pool of uniform liquid concentration was compared with the experimental mass transfer rate obtained previously. The results of this simulation first indicate that, for the mean length of the bubble's journey in the liquid phase of the reactor, the $CH_4$ and $CO_2$ content in the bubble is nearly constant, whereas the bubble is enriched in hydrogen. Second, the simulation results also predict that the change in bubble volume during its ascent would be minimal (the increase in diameter from bottom to top is usually less than 10%). This would then suggest that the bulk of the methane and carbon dioxide is transferred to the gas phase in a step before the rise of the bubble. In fact, it is conceivable that bubbles are formed in favorable nucleation sites (granules of biomass or microscopic solid particles), these sites being, in fact, surrounded by active biomass. The bubble formation rate (and hence the mass transfer rates for $CH_4$ and $CO_2$) would be intimately related to the biological activities of the biomass, and given the proximity of the nascent bubble to active biomass, the traditional diffusional barrier between the bubble and the bulk of the liquid phase would be less influential. Third, the $k_La$s expected during the ascent of the bubbles are low, but their values are consistent with experimental data for $H_2$ and can be predicted from first principles. Preliminary results, obtained in another UBF reactor, were in agreement with such simulation. The hydrogen partial pressures were 6.7 Pa in the gas phase of the reactor, while the bubbles of gas sampled from the liquid phase, just above the sludge bed, did not contain any detectable hydrogen. The methane and carbon dioxide partial pressures were 52.4 and 43.4 kPa, respectively, in the gas phase and 63.0 and 32.7 kPa, respectively, in the bubble sampled from the liquid phase. Future simulations and complementary analyses would clarify the mass transfer mechanisms in biomethanation.

## APPENDIX

**Material balance on a single bubble rising vertically in a homogeneous pool of liquid.** The mass balance of the three different gases on a single bubble was predicted, centimeter by centimeter during the

vertical ascent, with the assumptions of (i) an isolated bubble, (ii) no coalescence and no breakup, (iii) a vertical path at terminal velocity, (iv) all $c_i$s are constant w.r.t. time and uniform, (v) the interfacial area in the reactor is the same for all three gases, (vi) all the $H_2$ is transferred to the gas phase during the bubble ascent.

The calculation inputs were the bubble diameter and the three partial pressures at the surface as well as the actual dissolved-gas concentrations and the physical properties of the liquid. The mass transfer coefficients were obtained as outputs of the simulation, as was the profile for the partial pressure of the three gases as a function of the distance from the surface.

**Balances.** Partial with respect to each species (1 = $H_2$, 2 = $CH_4$, 3 = $CO_2$)

$$\frac{dn_i}{dt} = k_{Li} \cdot \pi d_B^2 \cdot (K_{Hi} p_i - c_i) \quad \text{(A1)}$$

where $d_B$ = bubble diameter (in centimeters), $k_{Li}$ = film coefficient for species $i$ (centimeters hour$^{-1}$), predicted by the Moo-Young Calderbank correlation (14), $n_i$ = number of moles of species $i$ in the bubble, $p_i$ = partial pressure of species $i$ (pascals), $c_i$ = molar concentration of species $i$ in the liquid pool (moles liter$^{-1}$), and $K_{Hi}$ = Henry's law constant for species $i$ (moles liter$^{-1}$ pascal$^{-1}$).

Using the ideal gas law ($p_i v_B = n_i RT$) and $v_B = (\pi d_B^3)/6$,

$$\frac{dp_i}{dt} = \frac{6RT}{d_B} k_{Li} (K_{Hi} p_i - c_i) - \frac{p_i}{v_B} \frac{dv_B}{dt} \quad \text{(A2)}$$

**Global balance.**

$$\frac{dn_{tot}}{dt} = \sum_{i=1}^{3} k_{Li} \pi d_B^2 (K_{Hi} p_i - c_i) \quad \text{(A3)}$$

Using the ideal gas law ($P_t v_B = n_{tot} RT$)

$$\frac{dv_B}{dt} = \frac{RT}{P_t} \pi d_B^2 \sum_{i=1}^{3} k_{Li} (K_{Hi} p_i - c_i) \quad \text{(A4)}$$

**Velocity.**

$$\frac{dh}{dt} = u_B \quad \text{(A5)}$$

where $h$ is the vertical distance from the surface and $u_B$ is the terminal velocity of the bubble. $u_B$ (14) is given by

TABLE A1. Summary of the simulation of the bubble ascent for the first steady state of the UBF reactor[a]

| Parameter | Value for: | | |
|---|---|---|---|
| | $H_2$ | $CH_4$ | $CO_2$ |
| $k_L$ (cm s$^{-1}$) | 0.02 | 0.01 | 0.01 |
| $k_L a$ (h$^{-1}$) | 0.40 | 0.19 | 0.19 |
| Partial pressure at the surface (Pa) | 49 | 11,600 | 89,681 |
| Partial pressure at $h$ = 66 cm (Pa) | 0 | 11,430 | 89,900 |
| Transfer rate attributed to ascent alone (mmol h$^{-1}$) | $7.38 \times 10^{-3}$ | 0.22 | 1.51 |
| Experimental transfer rate (mmol h$^{-1}$) | $7.38 \times 10^{-3}$ | 1.75 | 13.5 |
| Transfer rate attributed to bubble ascent (% of total rate) | 100 | 13 | 11 |

[a] Other salient data for the bubble ascent are as follows: bubble diameter at the surface, 0.38 cm; bubble diameter at $h$ = 66 cm, 0.37 cm; average bubble velocity, 23.9 cm s$^{-1}$; average bubble residence time, 3.35 s; total holdup for the reactor, $3.59 \times 10^{-4}$; interfacial area in the reactor, $5.79 \times 10^{-3}$ cm$^{-1}$.

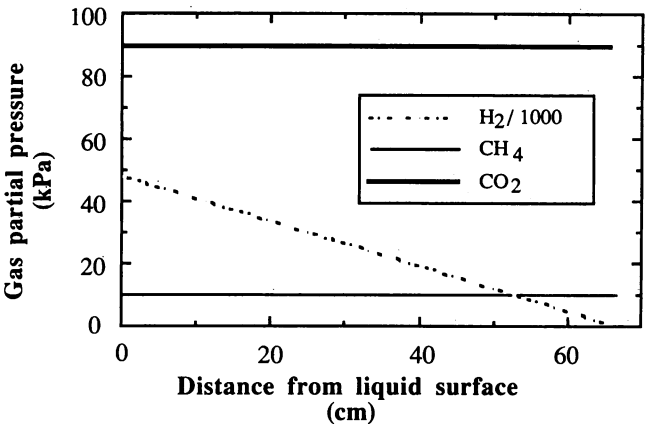


FIG. 6. Predicted partial pressures of hydrogen, methane, and carbon dioxide during the ascent of a single bubble in the UBF reactor (first steady state).

$$u_B = \sqrt{\frac{2\rho_L}{\sigma_L d_B} + \frac{g d_B}{2}} \quad \text{(A6)}$$

where $\rho_L$ and $\sigma_L$ are the specific density and surface tension of the liquid phase and $g$ is the gravitational acceleration.

**Integration.** Equations A2, A4, and A5 form a system of five first-order differential equations to be integrated starting from the liquid surface (direction opposite to physical phenomenon). Hence, the initial conditions are $h$ ($t$ = 0) = 0; $p_i$ ($t$ = 0) = experimental data on partial pressure; $v_B$ ($t$ = 0) = various real values corresponding to $0.05 \leq d_B \leq 0.5$ cm. Euler's method was used to integrate the system of equations with a $\Delta t$ of 0.1 s.

$$\frac{dy}{dt} = f(t,y) \text{ becomes } y(t_{n+1}) = y(t_n) + \Delta t \cdot f(t_n, y_n)$$

The results of the simulation of the first steady state of the UBF reactor are summarized in Table A1, and Fig. 6 presents the partial pressures of the three gases as a function of the distance from the surface.

The bubble ascent in the biomethanation process would then appear to be largely responsible for the removal of hydrogen from the liquid phase but is expected to have a very limited effect on its methane and carbon dioxide content. In turn, this means that the $CH_4$ and $CO_2$ contents of the gas phase would be much less subject to the interphase transfer resistance than the $H_2$ content.

## LITERATURE CITED

1. **Bailey, J. E., and D. F. Ollis.** 1986. Biochemical engineering fundamentals. McGraw-Hill Book Co., New York.
2. **Banta, A. P., and R. Pomeroy.** 1934. Hydrogen-ion concentration and $HCO_3^-$ concentration in digesting sludge. Sewage Works J. **6**:234–245.
3. **Beaubien, A., C. Jolicoeur, and J.-F. Alary.** 1988. Automated high sensitivity gas metering system for biological processes. Biotechnol. Bioeng. **32**:105–109.
4. **Boone, D. R., R. L. Johnson, and Y. Liu.** 1989. Diffusion of the interspecies electron carriers $H_2$ and formate in methanogenic ecosystems and its implications in the measurement of $K_m$ for $H_2$ or formate uptake. Appl. Environ. Microbiol. **55**:1735–1741.
5. **Conrad, R., and M. Babbel.** 1989. Effect of dilution on methanogenesis, hydrogen turnover and interspecies hydrogen transfer in anoxic paddy soil. FEMS Microbiol. Ecol. **62**:21–28.
6. **Danckwerts, P. V.** 1970. Gas-liquid reactions. *In* Chemical engineering series. McGraw Hill Book Co., New York.
7. **Demuynck, M., E. Nyns, and W. Palz.** 1983. Biogas plants in Europe. A practical handbook. Solar energy R&D in the European Community. Series E, vol. 6. D. Reidel, Dordrecht, The

Netherlands.

8. **Fardeau, M., and J. Belaich.** 1986. Energetics of the growth of *Methanococcus thermolithotrophicus*. Arch. Microbiol. **144:** 381–385.
9. **Fardeau, M., J. Peillex, and J. Belaich.** 1987. Energetics of the growth of *Methanobacterium thermoautotrophicum* and *Methanococcus thermolithotrophicus* on ammonium chloride and nitrogen. Arch. Microbiol. **148:**128–131.
10. **Harper, S. R., and F. G. Pohland.** 1986. Recent developments in hydrogen management during anaerobic biological wastewater treatment. Biotechnol. Bioeng. **28:**585–602.
11. **Knechtel, J. R.** 1978. A more economical method for the determination of chemical oxygen demand. Water Pollut. Control **116:**25–28.
12. **Lee, M. J., and S. H. Zinder.** 1988. Hydrogen partial pressures in a thermophilic acetate-oxidizing methanogenic culture. Appl. Environ. Microbiol. **54:**1457–1461.
13. **McInerney, M. J., and M. P. Bryant.** 1980. Basic principles of bioconversions in anaerobic digestion and methanogenesis, p. 277–296. *In* S. Sofer and O. Zaborsky (ed.), Biomass conversion processes for energy and fuels. Plenum Publishing Corp., New York.
14. **Moo-Young, M., and H. W. Blanch.** 1981. Design of biochemical reactors: mass transfer criteria for simple and complex systems. Adv. Biochem. Eng. **19:**1–69.

14a. **Pauss, A., R. Samson, S. R. Guiot, and C. Beauchemin.** 1990. Continuous measurement of dissolved $H_2$ in anaerobic digestion using a new hydrogen/air fuel cell probe. Biotechnol. Bioeng. **35:**492–501.

15. **Peillex, J., M. Fardeau, R. Boussand, J.-M. Navarro, and J. Belaich.** 1988. Growth of *Methanococcus thermolithotrophicus* in batch and continuous culture on $H_2$ and $CO_2$: influence of agitation. Appl. Microbiol. Biotechnol. **29:**560–564.
16. **Robinson, J. A., and J. M. Tiedje.** 1982. Kinetics of hydrogen consumption by rumen fluid, anaerobic sludge, and sediment. Appl. Environ. Microbiol. **44:**1374–1384.
17. **Scott, R. I., T. N. Williams, T. N. Whitmore, and D. Lloyd.** 1983. Direct measurement of methanogenesis in anaerobic digestors by membrane inlet mass spectrometry. Eur. J. Appl. Microbiol. Biotechnol. **18:**236–241.
18. **Seidell, A.** 1940. Solubilities of inorganic and metal organic compounds, 3rd ed. Van Nostrand Reinhold, New York.
19. **Sherwood, T. K., R. L. Pigford, and C. R. Wilke.** 1975. Mass transfer. *In* Chemical Engineering Series, McGraw Hill, New York.
20. **Smolenski, W. J., and J. Robinson.** 1988. In situ rumen hydrogen concentration in steers fed eight times daily, measured using a mercury reduction detector. FEMS Microbiol. Ecol. **53:**95–100.